Engine with unconventional crank mechanism FIK_1

Pavol Kukuča[1], *Dalibor* Barta[1,*] , *Robert* Labuda[1], *Tsvetomir* Gechev[2]

[1]University of Zilina, Department of Transport and Handling Machines, Faculty of Mechanical Engineering, Univerzitná 1, 010 26 Zilina, Slovakia
[2]Technical University – Sofia, Faculty of Transport, 8 Kliment Ohridski Blvd., Block 9, 1000 Sofia, Bulgaria

Abstract: The geometry and kinematics of unconventional engine mechanism FIK_1 are described in the paper. Transformation of the piston linear movement to rotational movement is done by a swinging board, a baseboard and a crankshaft. The paper describes the trajectory and acceleration of an observed point on the swinging board in all three planes as well as the kinematics of the piston movement. The principle of the unconventional mechanism FIK_1 is protected by patents No. 283742 and No. 283743. A mathematical model of the mechanism and some significant results are presented.

Keywords: Combustion engine, unconventional crank mechanism, kinematics, swinging board

1 Introduction

The effort to reduce the production costs of individual vehicle parts and to ensure their dimensional compactness while increasing reliability leads to the development of new structures and mechanisms. With the development and improvement of material and fuel technologies new and uncommon engines can also find application [1-4]. Some of these unconventional engines use an alternative construction of their mechanical parts and mechanisms to acquire certain advantages in comparison to the conventional solutions. A typical example is the axial engine for Stirling [5, 6] or IC application, which has a low frontal area, very good balance and great compactness [7-10]. Another unconventional type of engine mechanism which kinematics was solved by Shih [11] is the cycloidal internal combustion engine mechanism.

One of the mechanisms, applicable in such engines is the FIK_1, whose geometry and kinematics are described in this paper.

The base of the engine with unconventional mechanism is the swinging board D_K, supported on the crank pin and rolling by its perimeter around the immovable base board D_P (see Fig. 1, left) [12]. Both boards have an angle gearing at their perimeter (resp. at the optional suitable diameter) for exact and safe mutual rolling. The position of the gearing on

* Corresponding author: dalibor.barta@fstroj.uniza.sk

Reviewers: *Pawel* Drozdziel, *Saugirdas* Pukalskas

the base and swinging board may not be in praxis situated on their perimeters [13]. Because the swinging discs´ movement presents a relative consecutive rolling of two cones (see Fig. 1 right, there is shown the trajectory of a point on the swinging board perimeter, acquired from the virtual model), the gear can be positioned practically on the whole cone length from the bottom to the top.

The relative angle between both boards is φ (see Fig. 1, left). From the kinematics point of view this is the angle between the bottoms of the rolling boards. The top angle of the meshing cones does not need to be generally the same. In case of the identical cones their top angle value is (180° - φ).

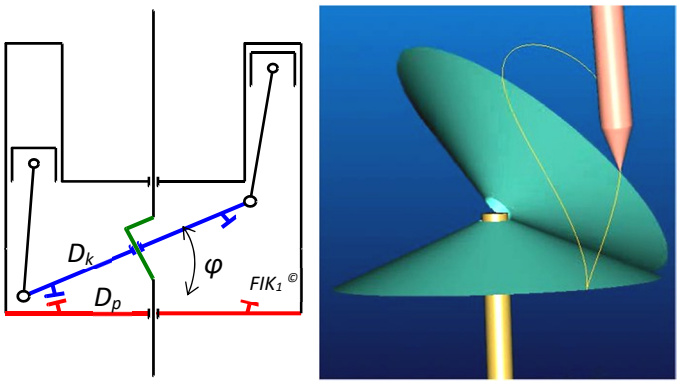

Fig. 1. Scheme of the unconventional engine mechanism

2 Description of the mechanism geometry

Based on the previous considerations, the center of the swinging board makes planar motion along a circle which is parallel to the plane of the immovable base board. Because each point on the swinging board makes a space movement, it is necessary to define and solve this system spatially (in three axes). We choose the coordinate system so that its vertical axis **Z** goes through the axis of the crank shaft and its center lies on the horizontal plane **XY** (see Fig. 2). The initial crank position for the rotation angle $\alpha = 0°$ lies on the axis **Y**. The observed point on the swinging board lies at the connecting line of the board center and its perimeter, it means opposite to the crank. The circle radius r_{kl}, which describes the center of the swinging board (hereinafter referred as "crank circle"), is given by the following expression:

$$r_{kl} = R \cdot (1 - \cos \phi), \tag{1}$$

where R – radius of the swinging (generating), resp. immovable base board,
φ - angle between boards which is equal to the crank angle (see Fig. 2).

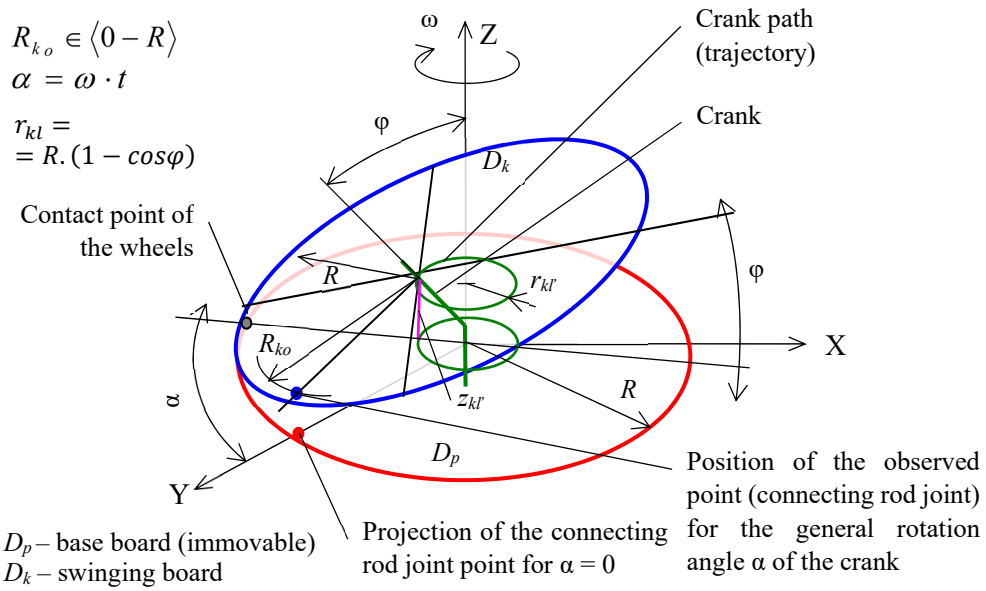

Fig. 2. Geometrical scheme of the unconventional mechanism FIK1

Distance between the planes of the crank circle and the immovable base board is given by expression

$$z_{kl'} = R \cdot \sin \phi \,. \tag{2}$$

By those assumptions each point of the swinging board, which lies outside of its center makes a general movement in three axes. In order to describe the kinematics of the piston movement, it is first necessary to describe the kinematics of a random point on the swinging board which lies on the radius R_{ko} (see Fig. 2), in the interval $R_{ko} \in \langle 0, R \rangle$. Further, it will be considered the possibility of changing the angle φ between both boards, which can theoretically be in the range $\varphi \in \langle 0, 90° \rangle$. Given the requirement, it is clear, that when the angle $\varphi = 0$ the swinging board makes no movement and when the angle φ is close to the 90°, then the engine design overall is unrealistic. Practically it is impossible to use higher angle values than 50°.

In relation to the piston movement it is most important to define mainly the vertical path of the random point on the swinging board (in direction of **Z** axis). This path, depending on the path of the point in the plane **XY** and on the connecting rod length, determines the value of the piston stroke which is in the direction of **Z** axis. According to the presented above, the path of the observed point on the swinging board in each axis depends on:

- radius R of the swinging, resp. base board,
- angle φ, between the planes of both boards,
- radius R_{ko}, where the observed point is located,
- rotation angle α of the crank as an independent variable.

3 Trajectory estimation of observed point on the swinging board

The path of the observed point is based upon a specific case when the angle value between both boards $\varphi = 90°$, the point lies on the perimeter of the swinging board i.e. $R_{ko} = R$, and the

crank shaft has the same crank angle $\varphi = 90°$. In such conditions the observed point performs a movement, whose projections to the individual axes (resp. planes) could be determined more simply, because the center of the swinging board is moving around the circle with a radius $r_{kl'} = R$. Its coordinates in four basic crank positions can be defined directly from the geometry of the physical model (Table 1).

Table 1. Position of the observed point

φ (◦)	α (◦)	x	y	z
90	0	0	R	0
	90	$-R$	R	R
	180	0	$-R$	$2R$
	270	R	R	R
	360	0	R	0

With so defined parameters the swinging board is situated permanently in the vertical plane and its perimeter is rolling around the perimeter of the immovable base board (see Fig. 3). At the same time the center of the swinging board describes a circle with radius $r_{kl'} = R$ in the horizontal plane (**XY**) at the height $z_{kl'} = R$. The crank is rotating around its axis with an angle α by an angular velocity ω.

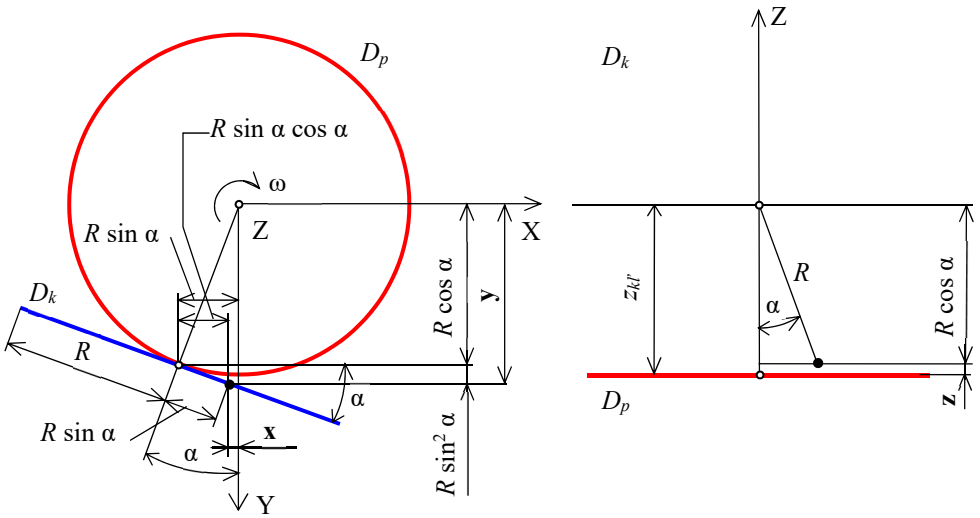

Fig. 3. System scheme for the angle φ = 90°

The position of the observed point at each random crank angle α can be determined from the geometric relationships with the following expressions (see Fig. 3):

$$x = R \cdot \sin\alpha \cdot (\cos\alpha - 1), \tag{3}$$

$$y = R \cdot (\cos\alpha + \sin^2\alpha), \tag{4}$$

$$z = R \cdot (1 - \cos\alpha). \tag{5}$$

If we want to observe movement of the point at an optional radius of the swinging board in the range of $R_{ko} \in \langle 0, R \rangle$, based on the similar consideration, by transforming (3), (4) and (5) we get expressions (6), (7) and (8):

$$x = \sin \alpha \cdot \left(R_{ko} \cdot \cos \alpha - R\right), \tag{6}$$

$$y = R \cdot \cos \alpha + R_{ko} \cdot \sin^2 \alpha , \tag{7}$$

$$z = R - R_{ko} \cdot \cos \alpha \cdot \tag{8}$$

In the next step, it is necessary to define the path of the observed point at the swinging board's perimeter ($R_{ko} = R$), provided that the angle φ between swinging and base board is random, but not 90°. Similar as in the previous case it is possible to simply define its location at four base locations of the crank from the physical model geometry. Values are presented in the Table 2.

Table 2. Position of the observed point

φ (◦)	α (◦)	x	y	z
≠90	0	0	R	0
	90	- $r_{kl'}$	R	R sin φ
	180	0	R - 2 $r_{kl'}$	2R sin φ
	270	$r_{kl'}$	R	R sin φ
	360	0	R	0

Even in this case, the swinging board, inclined under an angle φ, is rolling with its perimeter around the perimeter of the base board. The path of the observed point in the relation to the angle of the crank rotation α in each axis is affected by the inclination of the swinging board. Based on this, the path of the observed point in each axis is described by the following equations:

$$x = R \cdot \sin \alpha \cdot \left(\cos \alpha - 1\right) \cdot \left(1 - \cos \phi\right), \tag{9}$$

$$y = R \cdot \left(\cos \alpha + \sin^2 \alpha\right) \cdot \left(1 - \cos \phi\right) + R \cdot \cos \phi , \tag{10}$$

$$z = R \cdot \left(1 - \cos \alpha\right) \cdot \sin \phi \cdot \tag{11}$$

In the most general case, when the angle between the two boards φ is in the range $\varphi \in \langle 0, 90^\circ \rangle$ and the general point position on the swinging board D_K is in the range $R_{ko} \in \langle 0, R \rangle$ the expressions (9), (10) and (11) are presented in their universal form:

$$x = \sin \alpha \cdot \left(R_{ko} \cdot \cos \alpha - R\right) \cdot \left(1 - \cos \phi\right), \tag{12}$$

$$y = \left(R \cdot \cos \alpha + R_{ko} \cdot \sin^2 \alpha\right) \cdot \left(1 - \cos \phi\right) + R_{ko} \cdot \cos \phi , \tag{13}$$

$$z = \left(R - R_{ko} \cdot \cos \alpha\right) \cdot \sin \phi . \tag{14}$$

The following images show the visual interpretation of the solution of equations (12), (13) and (14) for one crank revolution and for the parameters of the physical model R = 0,1m,

R_{ko} = 0, 072m and φ = 30°. Graphical interpretation is done for each axis and in relation to the rotation angle of the crank α as well as in each of the three planes.

Fig. 4 shows the path of the observed point in the horizontal plane (**XY**). For better presentation the graph displays the half of the base board. Fig. 5 presents the path of the point in the vertical plane (**XZ**) and Fig. 6 – the point path in the vertical plane (**YZ**), whereas the axis of the engine cylinder is visible in the figure. The path of the observed point in all of the three axes in relation to the angle of the crank rotation α for one revolution is shown on the Fig. 7. The single curves indicate that the movement in the axes **X** and **Y** is inharmonic and movement in the axis **Z** is harmonic.

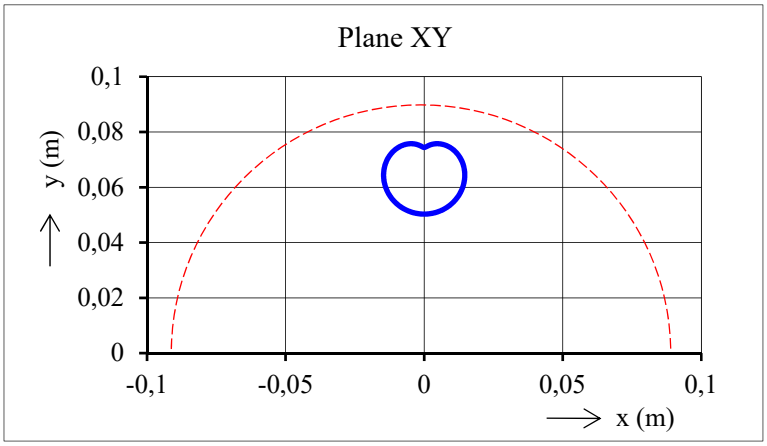

Fig. 4. Path of the observed point in the plane XY (shape of the immovable board is dashed)

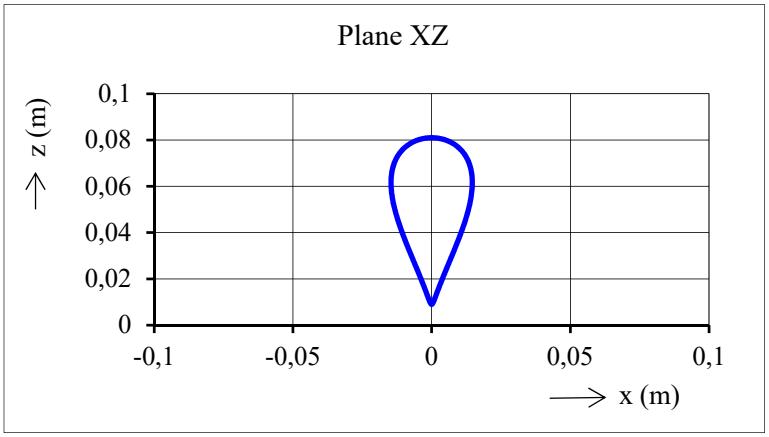

Fig. 5. Path of the observed point in the plane XZ

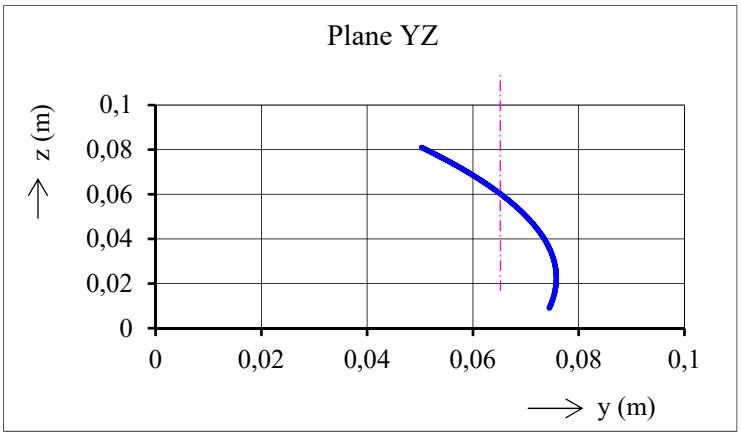

Fig. 6. Path of the observed point in the plane YZ (cylinder axis is dot-dashed)

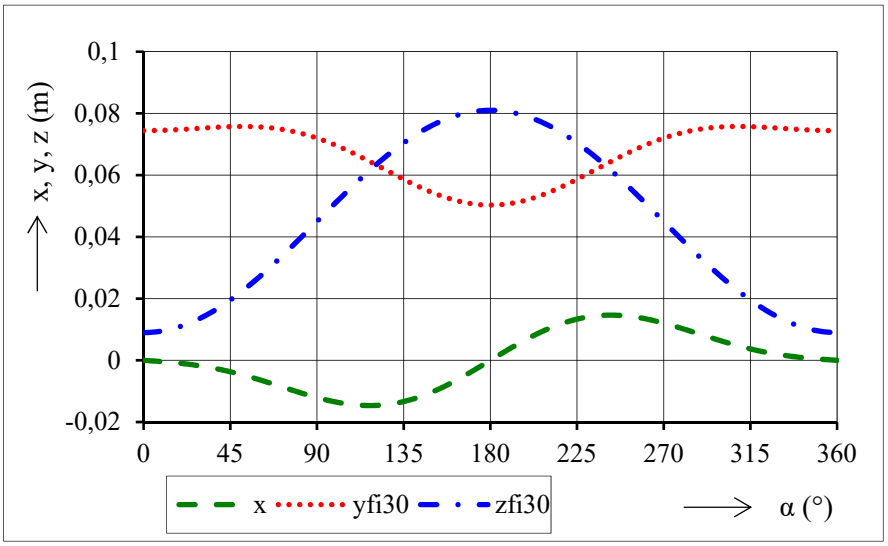

Fig. 7. Path of the observed point in relation to the angle of the crank rotation α

4 Velocity estimation of observed point

The velocity graphs of the observed point in each axis are obtained as a time derivative from the equations (12), (13) and (14). The following expressions represent them:

$$c_x = \frac{dx}{dt} = \frac{dx}{d\alpha} \cdot \frac{d\alpha}{dt} = \omega \cdot (1 - \cos\phi) \cdot \left[R_{ko} \cdot (1 - 2 \cdot \sin^2 \alpha) - R \cdot \cos\phi \right], \quad (15)$$

$$c_y = \frac{dy}{dt} = \frac{dy}{d\alpha} \cdot \frac{d\alpha}{dt} = \omega \cdot (1 - \cos\phi) \cdot (2 \cdot R_{ko} \cdot \sin\alpha \cdot \cos\alpha - R \cdot \sin\alpha), \quad (16)$$

$$c_z = \frac{dz}{dt} = \frac{dz}{d\alpha} \cdot \frac{d\alpha}{dt} = \omega \cdot R_{ko} \cdot \sin\alpha \cdot \sin\phi \cdot \quad (17)$$

Calculated velocities of the observed point on the swinging board in each of the three axes with crank revolutions n = 4000 min^{-1} are shown in the graph (Fig. 8). From the periodic and harmonic point of view, velocities have similar properties to paths.

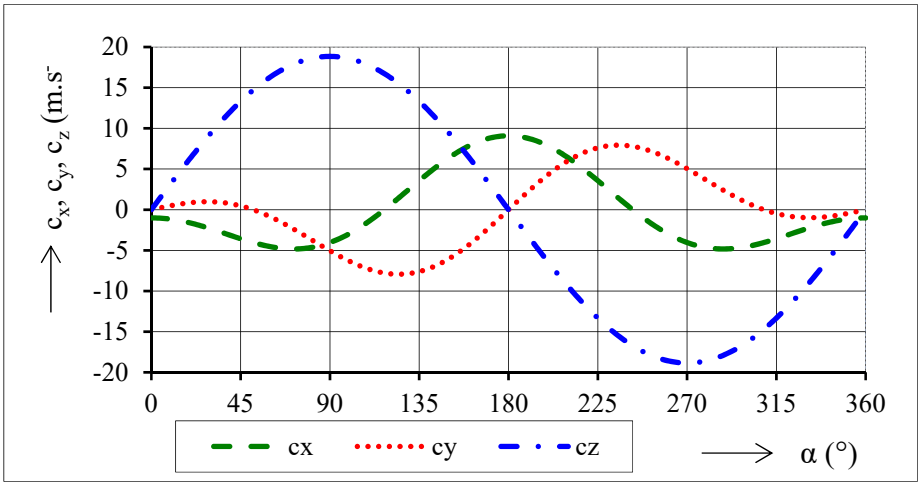

Fig. 8. Velocity of the observed point in relation to the angle of the crank rotation α

From the engine piston kinematics point of view, the dominant velocity is in the **Z** direction. Its maximal value is in the direction of cylinder axis and is about 4 m.s^{-1} higher, in comparison to the maximal velocity of the crank joint of a classical engine with comparable piston stroke. When calculating this velocity to the velocity of the piston, it must be taken into account, that the kinematics of the piston movement is affected by the wave movement of the connecting rod. Having a classic crank mechanism, the connecting rod makes the planar wave movement in the range equal to the piston stroke. In the case of engine with the swinging board, the connecting rod performs a spatial movement in significantly smaller range, in this case approximately only 40% of the piston stroke (see Fig. 4 and 6).

5 Acceleration of observed point

The acceleration graph of the observed point in each axis is obtained as the second derivative of equations (12), (13) and (14) with respect to time. After derivation and appropriate modification, the acceleration in axes X, Y, Z is:

$$a_x = \frac{d^2x}{dt^2} = \frac{d^2x}{d\alpha^2}\cdot\left(\frac{d\alpha}{dt}\right)^2 = \omega^2\cdot(1-\cos\phi)\cdot(R\cdot\sin\alpha - 4\cdot R_{ko}\cdot\sin\alpha\cdot\cos\alpha)\,, \quad (18)$$

$$a_y = \frac{d^2y}{dt^2} = \frac{d^2y}{d\alpha^2}\cdot\left(\frac{d\alpha}{dt}\right)^2 = \omega^2\cdot(1-\cos\phi)\cdot\left[2\cdot R_{ko}\cdot(1-2\cdot\sin^2\alpha) - R\cdot\cos\alpha\right], \quad (19)$$

$$a_z = \frac{d^2z}{dt^2} = \frac{d^2z}{d\alpha^2}\cdot\left(\frac{d\alpha}{dt}\right)^2 = \omega^2\cdot R_{ko}\cdot\cos\alpha\cdot\sin\phi\,, \quad (20)$$

Calculated accelerations of the observed point on the swinging board in each of the three axes with crank revolutions n = 4000 min^{-1} are shown in the graph (Fig. 9). From the periodic and harmonic point of view, accelerations have similar properties to paths or velocities.

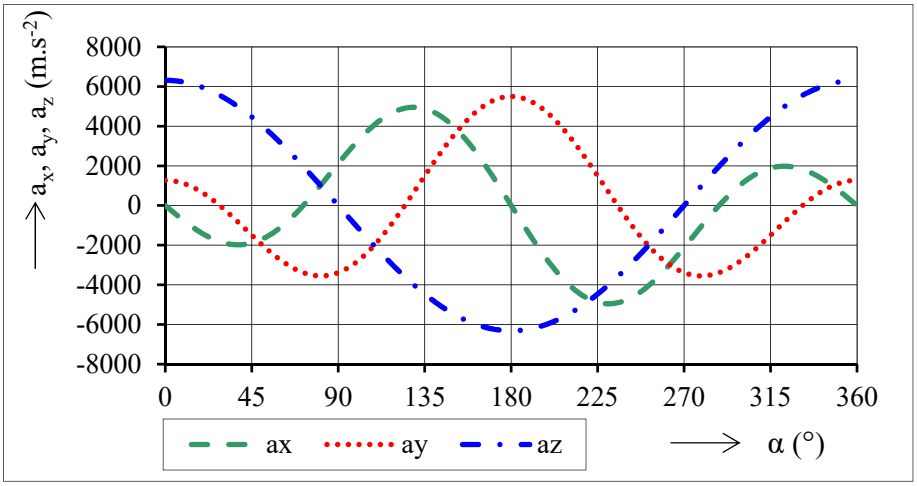

Fig. 9. Acceleration of the observed point in relation to the angle of the crank rotation α

In this case the dominant acceleration is in the Z direction as well. Its maximal value is in the direction of cylinder axis and is about 90 m.s^{-2} higher, in comparison to the maximal acceleration of the crank joint of a classical engine with comparable piston stroke. Percentagewise it is about 1,5% higher.

6 Conclusion

Based on the analytical result, that kinematics properties of the unconventional crank mechanism of the FIK$_1$ engine are comparable to the kinematics properties of the classical piston combustion engine with the same value of the piston stroke. It is possible to influence piston kinematics parameters by adjusting the distance of the cylinder axis from the axis of the crankshaft. A specific disadvantage of this mechanism is that the connecting rod performs a space movement, in contrast to the classical crank mechanism. That demands better design solution of its connection with the swinging board and piston.

This paper was realized as a part of the project KEGA 022ŽU-4/2017 – "Implementation of on-line education in the area of precise technologies with an impact on educational process to increase skills and flexibility of students of engineering fields of study" and as a result of the project implementation: "Modern methods of teaching of control and diagnostic systems of engine vehicles", ITMS code 26110230107, supported by the Operational Programme Education.

References

1. V. Morozov, A. Zhdanov, *Self-stopping actuating mechanism with high coefficient of efficiency of the forward stroke for linear motion drives*, MATEC Web of Conferences 75, 09001 (2016)
2. S. Erkaya, İ. Uzmay, *Experimental investigation of joint clearance effects on the dynamics of a slider-crank mechanism*, Multibody System Dynamics, vol. **24**, 1, p. 81–102, (2010)

3. S. J. Bo, T. C. Chen, Q. H. Ye, *Dynamics Research of rigid-flexible model of crank-rocker mechanism with Multi Clearance*, MATEC Web of Conferences **63**, 02027 (2016)
4. C. Toro, N. Lior, *Analysis and comparison of solar-heat driven Stirling, Brayton and Rankine cycles for space power generation*, Energy, vol. **120**, 549-564, (2017)
5. P. Baran, P. Kukuča, D. Barta, *Simulations of non-convetional mechanisms for stirling engine,* Proceeding of BulTrans – 2014, 167, (2014)
6. P. Baran, P. Stastniak, M. Brezani, *Dynamic analysis and comparison of balancing systems of nonconventional piston machine FIK1*. Proceeding of conference: Dynamics of rigid and deformable bodies 2016,. 9-15, (2016)
7. *Axial Internal – Combustion Engines*, http://www.douglasself.com/MUSEUM/POWER/unusualICeng/axial-ICeng/axial-IC.htm, (2008)
8. E. García-Cansecoa, A. Alvarez-Aguirreb, J. M.A. Scherpenc, *Modeling for control of a kinematic wobble-yoke Stirling engine*, Renewable Energy, vol. **75**, 808-817, (2015)
9. Yu. Pogulyaev, O. Nikishin, A. Zheltov, *The kinematics of the swashplate engine with two rotating pairs*, Procedia Engineering, vol. **206**, 1722-1727, (2017)
10. Ł. Jedliński, J. Caban, L. Krzywonos, S. Wierzbicki, F. Brumerčik, *Application of vibration signal in the diagnosis of IC engine valve clearance,.* VP, vol. **3**, 14-19, (2014)

A. J. Shih, *Kinematics of the Cycloidal Internal Combustion Engine Mechanism,* Journal of mechanical design, vol. **115 (4)**, p. 953-959, (2008)

11. P. Fitz, R. Isteník, P. Kukuča, *Mechanizmus piestového stroja*, Vestník ÚPV SR, patent č. 283743**,** (12/2003)
12. R. Isteník, *Simulácia mechanických a termomechanických procesov v spaľovacích motoroch a vozidlách*, Habilitačná práca, KKVMZ SjF Žilinská univerzita, (2002)